

Effect of diverse solvents on the composition and structure of mixed-ligand nickel(II) dithiocarbamates: $[\text{NiX}(\text{ndtc})(\text{PPh}_3)]$



Richard Pastorek^a, Pavel Štarha^b, Bohuslav Drahoš^b, Zdeněk Trávníček^{b,*}

^a Department of Inorganic Chemistry, Faculty of Science, Palacký University, 17, listopadu 12, CZ-771 46 Olomouc, Czech Republic

^b Regional Centre of Advanced Technologies and Materials, Department of Inorganic Chemistry, Faculty of Science, Palacký University, 17. listopadu 12, CZ-771 46 Olomouc, Czech Republic

ARTICLE INFO

Article history:

Received 3 September 2013

Accepted 30 November 2013

Available online 12 December 2013

Keywords:

Nickel(II) complexes

Dithiocarbamate

Crystal structure

Solution study

NMR

Mass spectrometry

ABSTRACT

A series of square-planar nickel(II) benzylpiperazine–dithiocarbamate (*bpdtc*; **1–4**) and thiomorpholine–dithiocarbamate (*tmdtc*; **5–8**) complexes of the composition $[\text{NiX}(\text{ndtc})(\text{PPh}_3)]$ (*X* symbolizes Cl for **1** and **5**, Br for **2** and **6**, I for **3** and **7**, or NCS for **4** and **8**) was prepared and thoroughly characterized by elemental analysis, UV–Vis, IR and NMR spectroscopy, mass spectrometry, molar conductivity and magnetochemical measurements, and by single-crystal X-ray analysis (for complex **1**). The solution behaviour study of selected representatives (**1**, **4**, **5** and **8**) in various solvents (acetone, acetonitrile, methanol (MeOH), *N,N*-dimethylformamide (DMF), chloroform, nitromethane, dimethyl sulfoxide (DMSO), MeOH/water mixture (1:1 v/v)) by a combination of NMR and UV–Vis spectroscopy, mass spectrometry and single-crystal X-ray analysis showed that the complexes decompose back to the synthetic precursors, involving the $[\text{Ni}(\text{ndtc})_2]$ species, in DMF and DMSO, while they dissolve without a change in their composition in the remaining solvents.

© 2013 Elsevier Ltd. All rights reserved.

1. Introduction

S-donor ligands bearing the dithiocarbamate moiety are commonly used for the preparation of transition metal complexes having various compositions, geometries, properties and applications. For example, complexes involving this type of ligand were reported in the literature as having interesting electrochemical [1], antibacterial (higher than tetracycline), antifungal (higher than nystatin) [2] and antitumor activities (higher *in vitro* and *in vivo* activities as compared with *cisplatin*) [3] or they may act as precursors for the preparation of NiS nanoparticles [4]. On the other hand, the dithiocarbamates presented in this work, *i.e.* benzylpiperazine–dithiocarbamate (*bpdtc*) and thiomorpholine–dithiocarbamate (*tmdtc*), are quite rare, since the literature sources contain only 11 transition metal complexes with *bpdtc* and 41 with *tmdtc* (SciFinder[®], 2013). As for the nickel(II) complexes with the above-mentioned dithiocarbamates, $[\text{Ni}(\text{bpdtc})_2]$ [5], $[\text{Ni}(\text{bpdtc})(\text{phen})_2]\text{ClO}_4\cdot\text{CHCl}_3$, $[\text{Ni}(\text{bpdtc})(\text{phen})_2]\text{SCN}$ [6], $[\text{Ni}(\text{tmdtc})_2]$ [7] and $[\text{Ni}(\text{en})_3(\text{tmdtc})_2]$ [8] have been reported to date. Regarding the X-ray structures determined for transition metal complexes with the *bpdtc* and *tmdtc* ligands, only three, *i.e.* $[\text{Ni}(\text{bpdtc})(\text{phen})_2]\text{ClO}_4\cdot\text{CHCl}_3$ [6], $[\text{MoO}_2(\text{tmdtc})_2]$ [9] and $[\text{Ni}(\text{bpdtc})(\text{PPh}_3)_2]\text{ClO}_4\cdot\text{PPh}_3$ [10], have been deposited with the Cambridge Structural Database (CSD ver. 5.34, May 2013 update [11]).

This work reports solid-state and solutions studies on a series of nickel(II) benzylpiperazine– and thiomorpholine–dithiocarbamate complexes of the type $[\text{NiX}(\text{ndtc})(\text{PPh}_3)]$, whose coordination sphere consists of a bidentate-coordinated S-donor dithiocarbamate anion, one PPh_3 molecule and one of the Cl^- , Br^- , I^- or NCS^- ligands, denoted as *X*, and having an S_2PX donor set. The main benefit of this work is that it provides different perspectives on mixed-ligand nickel(II)–dithiocarbamate complexes in connection with their solution properties, specifically it describes their behaviour upon dissolving in various solvents. These findings may play a significant role in a broader context of possible practical applications of nickel dithiocarbamates.

2. Experimental

2.1. Materials

Chemicals and solvents used in this work were purchased from Sigma–Aldrich Co. (*N*-benzylpiperazine, thiomorpholine, triphenylphosphine), Fluka Co. (CS_2) and Lachema Co. (solvents). $[\text{Ni}(\text{bpdtc})_2]$, $[\text{Ni}(\text{tmdtc})_2]$ and $[\text{NiX}_2(\text{PPh}_3)_2]$ were prepared as formerly described elsewhere [5,7,12]; *X* = Cl^- , Br^- , I^- , NCS^- .

2.2. Syntheses of the complexes

The starting nickel(II) complexes $[\text{Ni}(\text{ndtc})_2]$ (1 mmol) and $[\text{NiX}_2(\text{PPh}_3)_2]$ (1 mmol) were pulverized and mixed together in

* Corresponding author. Tel.: +420 585 634 352; fax: +420 585 634 954.

E-mail address: zdenek.travnicek@upol.cz (Z. Trávníček).

20 mL of CHCl_3 . The suspension was stirred until dissolved (ca. 45 min) and then 1 mg of activated charcoal was added. The mixture was filtered off and diethyl ether (ca. 3 mL) was poured into the filtrate and left to crystallize for two days (*note*: in the case that crystals did not form after two days, another portion of diethyl ether was added and the solution was left to crystallize). Microcrystals of $[\text{NiX}(\text{ndtc})(\text{PPh}_3)]$ (**1–8**; Scheme 1) were filtered off and washed with diethyl ether (3×5 mL) and dried at 40°C under an infrared lamp. Crystals suitable for single-crystal X-ray analysis were obtained as follows: complex **1** was dissolved in CHCl_3 , the solution was filtered and left to stand in a refrigerator, where dark violet crystals formed after a few days.

$[\text{NiCl}(\text{bpdtc})(\text{PPh}_3)]$ (**1**): Light violet crystals. Yield: 66%. *Anal.* Calc. for $\text{C}_{30}\text{H}_{30}\text{N}_2\text{ClNiPS}_2$: C, 59.28; H, 4.97; N, 4.61; Cl, 5.83; Ni, 9.66. Found: C, 58.86; H, 5.01; N, 4.70; Cl, 6.25; Ni, 9.71%. λ_{M} ($\text{MeNO}_2/\text{MeCN}$; $\text{S cm}^2 \text{ mol}^{-1}$): 2.2/14.0. UV–Vis ($\text{Me}_2\text{CO}/\text{MeCN}/\text{CHCl}_3$ solution; $\times 10^3 \text{ cm}^{-1}$): 19.5/19.6/19.4. ϵ_{max} ($\text{Me}_2\text{CO}/\text{MeCN}/\text{CHCl}_3$ solution; $\text{M}^{-1} \text{ cm}^{-1}$): 472.2/504.9/459.9.

$[\text{NiBr}(\text{bpdtc})(\text{PPh}_3)]$ (**2**): Dark violet crystals. Yield: 62%. *Anal.* Calc. for $\text{C}_{30}\text{H}_{30}\text{N}_2\text{BrNiPS}_2$: C, 55.24; H, 4.64; N, 4.29; Br, 12.25; Ni, 9.00. Found: C, 54.87; H, 4.60; N, 4.44; Br, 12.51; Ni, 9.11%. λ_{M} (MeNO_2 ; $\text{S cm}^2 \text{ mol}^{-1}$): 2.4.

$[\text{NiI}(\text{bpdtc})(\text{PPh}_3)]$ (**3**): Light violet crystals. Yield: 54%. *Anal.* Calc. for $\text{C}_{30}\text{H}_{30}\text{N}_2\text{INiPS}_2$: C, 51.53; H, 4.32; N, 4.01; Ni, 8.39. Found: C, 51.26; H, 4.50; N, 4.13; Ni, 8.18%. λ_{M} (MeNO_2 ; $\text{S cm}^2 \text{ mol}^{-1}$): 2.3.

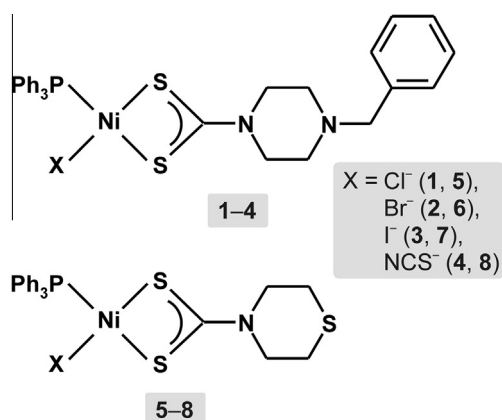
$[\text{Ni}(\text{NCS})(\text{bpdtc})(\text{PPh}_3)]$ (**4**): Light red crystals. Yield: 57%. *Anal.* Calc. for $\text{C}_{31}\text{H}_{30}\text{N}_3\text{NiPS}_3$: C, 59.06; H, 4.80; N, 6.67; Ni, 9.31. Found: C, 58.78; H, 4.40; N, 6.62; Ni, 9.43%. λ_{M} (MeNO_2 ; $\text{S cm}^2 \text{ mol}^{-1}$): 2.6.

$[\text{NiCl}(\text{tmdtc})(\text{PPh}_3)] \cdot \frac{1}{2}\text{CHCl}_3$ (**5**): Dark violet crystals. Yield: 68%. *Anal.* Calc. for $\text{C}_{23}\text{H}_{23}\text{NClNiPS}_3 \cdot \frac{1}{2}\text{CHCl}_3$: C, 47.48; H, 3.98; N, 2.36; Cl, 14.91; Ni, 9.87. Found: C, 46.98; H, 3.93; N, 2.56; Cl, 14.43; Ni, 10.08%. λ_{M} ($\text{MeNO}_2/\text{MeCN}$; $\text{S cm}^2 \text{ mol}^{-1}$): 3.3/20.5. UV–Vis ($\text{Me}_2\text{CO}/\text{MeCN}/\text{CHCl}_3$ solution; $\times 10^3 \text{ cm}^{-1}$): 19.4/19.5/19.4. ϵ_{max} ($\text{Me}_2\text{CO}/\text{MeCN}/\text{CHCl}_3$ solution; $\text{M}^{-1} \text{ cm}^{-1}$): 570.6/763.1/452.8.

$[\text{NiBr}(\text{tmdtc})(\text{PPh}_3)] \cdot \frac{1}{2}\text{CHCl}_3$ (**6**): Dark violet crystals. Yield: 63%. *Anal.* Calc. for $\text{C}_{23}\text{H}_{23}\text{NBrNiPS}_3 \cdot \frac{1}{2}\text{CHCl}_3$: C, 44.18; H, 3.71; N, 2.19; X, 12.51; Ni, 9.19. Found: C, 44.01; H, 3.53; N, 2.25; X, 12.03; Ni, 9.47%. X = Br + Cl. λ_{M} (MeNO_2 ; $\text{S cm}^2 \text{ mol}^{-1}$): 3.2.

$[\text{NiI}(\text{tmdtc})(\text{PPh}_3)] \cdot \frac{1}{2}\text{CHCl}_3$ (**7**): Dark brown crystals. Yield: 55%. *Anal.* Calc. for $\text{C}_{23}\text{H}_{23}\text{NINiPS}_3 \cdot \frac{1}{2}\text{CHCl}_3$: C, 41.15; H, 3.45; N, 2.04; Ni, 8.56. Found: C, 41.52; H, 3.13; N, 2.29; Ni, 8.89%. λ_{M} (MeNO_2 ; $\text{S cm}^2 \text{ mol}^{-1}$): 3.6.

$[\text{Ni}(\text{NCS})(\text{tmdtc})(\text{PPh}_3)]$ (**8**): Light red crystals. Yield: 51%. *Anal.* Calc. for $\text{C}_{24}\text{H}_{23}\text{N}_2\text{NiPS}_4$: C, 51.72; H, 4.16; N, 5.03; Ni, 10.53. Found: C, 51.34; H, 3.72; N, 4.90; Ni, 10.37%. λ_{M} (MeNO_2 ; $\text{S cm}^2 \text{ mol}^{-1}$): 2.9.



Scheme 1. Structural formulas of the studied complexes.

2.3. Physical methods

Elemental analyses (C, H, N) were performed on a Flash 2000 CHNO-S Analyser (Thermo Scientific). Chlorine and bromine contents were determined using the Schöniger method. The nickel content was determined by chelatometric titration with murexide as an indicator. The measurements of the room temperature magnetic susceptibilities were performed using the Faraday method with a laboratory designed instrument and with a Sartorius 4434 MP-8 microbalance. $\text{Co}[\text{Hg}(\text{NCS})_4]$ was used as a calibrant and the correction for diamagnetism was performed using Pascal constants [13]. The molar conductivity of the 10^{-3} M nitromethane (MeNO_2 ; **1–8**) and acetonitrile (MeCN ; **1, 5**) solutions was measured by an LF 330/SET conductometer (WTW GmbH) at 25°C . Electronic absorption spectra (10^{-3} M solutions in acetone (Me_2CO), MeCN , *N,N*-dimethylformamide (DMF), dimethyl sulfoxide (DMSO), chloroform (CHCl_3) and MeNO_2); the complexes were not soluble in methanol (MeOH), ethanol (EtOH) and water up to the 10^{-3} M concentration) and diffuse-reflectance spectra were recorded on a Lambda 40 spectrometer (Perkin-Elmer) in the range 200–1000 nm. IR spectra ($450\text{--}4000 \text{ cm}^{-1}$ region; KBr pellets) were recorded on a Perkin-Elmer Spectrum one FT-IR spectrometer. ^{31}P NMR spectra of CDCl_3 (**1–8**) and $\text{DMSO}-d_6$ (**1, 5**) solutions were measured at 300 K on a Varian 400 MHz NMR device and the spectra were calibrated against the signals of 85% H_3PO_4 , used as an external standard. Mass spectra of solutions of **1, 4, 5** and **8** in Me_2CO , MeCN , MeOH , DMF, CHCl_3 , MeNO_2 , and a $\text{MeOH}/\text{H}_2\text{O}$ mixture (1:1 v/v), and $[\text{Ni}(\text{ndtc})_2]$ and $[\text{NiCl}_2(\text{PPh}_3)_2]$ in DMF were recorded on an LCQ Fleet Ion Mass Trap spectrometer (Thermo Scientific Inc.) using the electro-spray ionization technique in the positive mode (ESI+).

2.4. Crystal structure determinations

A series of attempts to re-crystallize selected representatives (**1, 4, 5** and **8**) from different solvents (Me_2CO , MeCN , MeOH , CHCl_3 , MeNO_2) with the aim to obtain crystals suitable for single crystal X-ray analysis was performed. We were successful in the case of re-crystallization of complex **1** from CHCl_3 , which led to the formation of well-shaped dark violet single crystals of which one was used for the diffraction experiment. On the other hand, slow cooling of hot (80°C) DMF or DMSO solutions of **1, 4, 5** and **8**, as well as slow evaporation of DMF solutions of **1, 4, 5** and **8** at room temperature led to uniform crystalline products, whose compositions corresponded to the starting compounds $[\text{Ni}(\text{bpdtc})_2]$ and $[\text{Ni}(\text{tmdtc})_2]$, as proven by elemental analysis, mass spectrometry and X-ray analysis. The crystals obtained by slow evaporation of a DMF solution of **1** and by cooling of a hot DMSO solution of **8** were selected as representatives of both groups of products (*i.e.* $[\text{NiX}(\text{bpdtc})(\text{PPh}_3)]$ (**1–4**) and $[\text{NiX}(\text{tmdtc})(\text{PPh}_3)]$ (**5–8**)), differing in the *ndtc* ligand.

The single-crystal X-ray analyses of selected crystals of $[\text{NiCl}(\text{bpdtc})(\text{PPh}_3)]$ (**1**), $[\text{Ni}(\text{bpdtc})_2]$ and $[\text{Ni}(\text{tmdtc})_2]$ were collected on an XcaliburTM2 diffractometer (Oxford Diffraction Ltd.) with a Sapphire2 CCD detector and with $\text{Mo K}\alpha$ radiation (Monochromator Enhance, Oxford Diffraction Ltd.). Data collection and reduction were performed using the CRYSDALS software [14]. This software was also used for data correction for absorption effects (empirical absorption correction using spherical harmonics) implemented in the SCALE3 ABSPACK scaling algorithm. The structures were solved by direct methods (SHELXS-97) and refined on F^2 using the full-matrix least-squares procedure by SHELXL-97 [15]. Non-hydrogen atoms were refined anisotropically. Hydrogen atoms were located in a difference map and refined by the riding model: $\text{C–H} = 0.95$ (CH) and 0.99 (CH_2) Å, and $U_{\text{iso}}(\text{H}) = 1.2 U_{\text{eq}}(\text{CH}, \text{CH}_2)$. Atoms of one phenyl ring of a PPh_3 molecule of **1** are disordered

Table 1
Crystal data and structure refinement for [Ni(*bpdtc*)₂], [Ni(*tmdtc*)₂] and [NiCl(*bpdtc*)(PPh₃)] (**1**).

	[Ni(<i>bpdtc</i>) ₂]	[Ni(<i>tmdtc</i>) ₂]	[NiCl(<i>bpdtc</i>)(PPh ₃)] (1)
Empirical formula	C ₂₄ H ₃₀ N ₄ S ₄ Ni	C ₁₀ H ₁₆ N ₂ S ₆ Ni	C ₃₀ H ₃₀ N ₂ ClNiPS ₂
Formula weight	561.47	415.32	607.81
<i>T</i> (K)	120(2)	120(2)	120(2)
λ (Å)	0.71073	0.71073	0.71073
Crystal system	monoclinic	monoclinic	triclinic
Space group	<i>P</i> 2 ₁ / <i>n</i>	<i>P</i> 2 ₁ / <i>n</i>	$\bar{P}1$
<i>Unit cell dimensions</i>			
<i>a</i> (Å)	12.9570(4)	4.4296(2)	9.9872(3)
<i>b</i> (Å)	6.5281(2)	20.8438(6)	10.8573(3)
<i>c</i> (Å)	31.1594(10)	8.4902(2)	13.2971(3)
α (°)	90	90	95.342(2)
β (°)	96.210(3)	97.055(3)	93.702(2)
γ (°)	90	90	93.677(2)
<i>V</i> (Å ³)	2620.2(2)	777.97(4)	1429.04(6)
<i>Z</i>	4	2	2
<i>D</i> _{calc} (g cm ⁻³)	1.423	1.773	1.413
Absorption coefficient (mm ⁻¹)	1.079	2.038	0.997
Crystal size (mm)	0.25 × 0.20 × 0.10	0.20 × 0.15 × 0.10	0.25 × 0.25 × 0.10
<i>F</i> (000)	1176	428	632
θ range for data collection (°)	3.16 ≤ θ ≤ 25.00	3.11 ≤ θ ≤ 24.99	3.08 ≤ θ ≤ 25.00
Index ranges (<i>h, k, l</i>)	−15 ≤ <i>h</i> ≤ 12 −7 ≤ <i>k</i> ≤ 7 −37 ≤ <i>l</i> ≤ 37	−5 ≤ <i>h</i> ≤ 4 −24 ≤ <i>k</i> ≤ 24 −10 ≤ <i>l</i> ≤ 10	−11 ≤ <i>h</i> ≤ 11 −12 ≤ <i>k</i> ≤ 11 −15 ≤ <i>l</i> ≤ 15
Reflections collected/unique (<i>R</i> _{int})	23547/4613 (0.0238)	7123/1365 (0.0256)	14135/5000 (0.0325)
Data/restraints/parameters	4613/0/289	1365/0/88	5000/66/384
Goodness-of-fit (GOF) on <i>F</i> ²	1.009	1.084	0.958
Final <i>R</i> indices [<i>I</i> > 2 σ (<i>I</i>)]	<i>R</i> ₁ = 0.0293 <i>wR</i> ₂ = 0.0824	<i>R</i> ₁ = 0.0221 <i>wR</i> ₂ = 0.0544	<i>R</i> ₁ = 0.0333 <i>wR</i> ₂ = 0.0694
<i>R</i> indices (all data)	<i>R</i> ₁ = 0.0627 <i>wR</i> ₂ = 0.0859	<i>R</i> ₁ = 0.0283 <i>wR</i> ₂ = 0.0554	<i>R</i> ₁ = 0.0511 <i>wR</i> ₂ = 0.0721
Largest peak and hole (e Å ⁻³)	0.363, −0.195	0.363, −0.204	0.467, −0.550

over two positions with occupancy factors of 0.52, and 0.48. The crystal data and structure refinements are given in Table 1. The molecular graphics were drawn and additional structural calculations were interpreted with DIAMOND software [16].

3. Results

3.1. General properties

The composition of the prepared complexes correlates with the results of the elemental analyses (the differences between the calculated and found contents were not higher than 0.50%). The magnetochemical experiments proved the complexes to be diamagnetic, which corresponds with a square-planar geometry of the nickel(II) complexes. The molar conductivity values of **1–8** dissolved in MeNO₂ were found to be in the range 2.2–3.6 S cm² mol⁻¹, which are characteristic values for non-electrolytes in the solvent used [17]. The maxima of the $\nu(\text{C}\cdots\text{S})$ and $\nu(\text{C}\cdots\text{N})$ vibrations, characteristic for the dithiocarbamate moiety, were detected in the IR spectra of all the complexes at 995–998 and 1507–1531 cm⁻¹, respectively (Table 2) [18,19]. The IR spectra of **4** and **8** also contain the bands of the $\nu(\text{C}=\text{S})$ (maximum at 844 cm⁻¹ for **4** and 839 cm⁻¹ for **8**) and $\nu_{\text{as}}(\text{C}=\text{N})$ (maximum at 2090 cm⁻¹ for **4** and 2098 cm⁻¹ for **8**) vibrations, indirectly showing the coordination of the NCS⁻ group to nickel(II) through the nitrogen atom [20,21].

3.2. X-ray structure of [NiCl(*bpdtc*)(PPh₃)] (**1**), [Ni(*bpdtc*)₂] and [Ni(*tmdtc*)₂]

The complex [NiCl(*bpdtc*)(PPh₃)] (**1**), with a distorted square-planar geometry, consists of a central Ni(II) atom tetra-coordinated by two sulfur atoms (a bidentate-coordinated *bpdtc* anion), one

phosphorus atom of the PPh₃ molecule and one chloride anion, giving a CIPS₂ donor set (Fig. 1, Table 3). One phenyl ring of the PPh₃ molecule is distorted over two positions with occupancy factors of 0.520(5) and 0.480(5). The bond lengths around the metal centre, given in Table 3, were compared with those of nine formerly reported [NiCl(*ndtc*)(PPh₃)] complexes [22–30] involving different dithiocarbamate ligands. In the case of Ni–S (2.171–2.231 Å range, average value based on a CSD search: 2.202 Å; Ni–S = 2.1724(7) and 2.2181(6) Å for **1**) and Ni–P (2.185–2.224 Å range, average value based on a CSD search: 2.202 Å; Ni–P = 2.2029(6) Å for **1**), the values of **1** fall into reported ranges. However, the Ni–Cl bond length of **1** (2.1627(7) Å) was found to be shorter as compared with previously reported analogous nickel(II) dithiocarbamate complexes (2.174–2.195 Å range, average value based on a CSD search: 2.184 Å).

The crystal structure of **1** (Fig. 2) is stabilised by a network of non-covalent contacts of the C–H \cdots Cl, C–H \cdots S, C–H \cdots π and C–H \cdots C types, thus forming a 3D supramolecular architecture, in which two adjacent molecules are centrosymmetrically connected through the C4–H \cdots S2 interactions. Selected parameters of the non-covalent contacts are as follows: C2–H2B \cdots C1 with *d*(D \cdots A) = 3.718(4) Å; C4–H4B \cdots S2 with *d*(D \cdots A) = 3.897(2) Å; C6–H6A \cdots Cg with *d*(D \cdots A) = 3.552(2) Å; C23–H23A \cdots S2 with *d*(D \cdots A) = 3.704(2) Å; C32–H32A \cdots C10 with *d*(D \cdots A) = 3.526(6) Å; C42–H42A \cdots C11 with *d*(D \cdots A) = 3.473(2) Å. Detailed information about the above discussed non-covalent contacts is given in Table S1 in Appendix A, Supplementary data.

The molecular structures of both [Ni(*bpdtc*)₂] and [Ni(*tmdtc*)₂] are centrosymmetric (Fig. S1 in Appendix A, Supplementary data). [Ni(*bpdtc*)₂] involves two halves of crystallographically independent molecules within the unit cell, with a Ni \cdots Ni separation of 6.4785(2) Å. The Ni(II) atoms are tetra-coordinated by four sulfur atoms of two *bpdtc* ligands (Table 3). The determined Ni–S bond lengths of [Ni(*bpdtc*)₂] and [Ni(*tmdtc*)₂] (Table 3) do not differ from

Table 2

Selected NMR, IR and electronic (diffuse-reflectance and solution absorption spectra of 10^{-3} M nitromethane (MeNO₂), *N,N'*-dimethylformamide (DMF) and dimethyl sulfoxide (DMSO) solutions) spectral data for **1–8**.

Complex	³¹ P NMR (ppm)	IR (cm ⁻¹) ^a		Uv-Vis ($\times 10^3$ cm ⁻¹)		
		$\nu(\text{C}\cdots\text{S})$	$\nu(\text{C}\cdots\text{N})$	Diffuse-reflectance	MeNO ₂ ^b	DMF ^c
1	20.7	995m	1521s	19.5, 28.3, 41.1	19.6 (443.2)	15.8, 21.2
2	23.6	995m	1520s	19.1, 27.9, 40.9	19.4 (387.9)	15.7, 21.2
3	29.0	996m	1524s	18.6, 29.8, 36.3, 44.9	19.2 (370.7)	15.7, 21.2sh
4	29.4	996m	1531s	20.9, 29.9, 40.7	20.9 (795.2)	15.7, 21.3
5	36.3	996m	1528s	19.7, 29.7, 41.7	19.5 (620.7)	15.8, 21.2sh
6	44.3	997m	1518s	19.0, 27.9, 40.2	19.2 (481.8)	15.8, 21.1sh
7	40.4	997m	1507s	18.4, 27.8, 43.6	18.9 (286.3)	15.8, 21.2sh
8	34.0	998m	1518s	20.3, 28.1, 42.6	20.8 (884.1)	15.8, 21.2sh

^a m = middle intensity; s = strong intensity.

^b the values of molar absorption coefficients are in parentheses ($\text{M}^{-1} \text{cm}^{-1}$).

^c sh = shoulder.

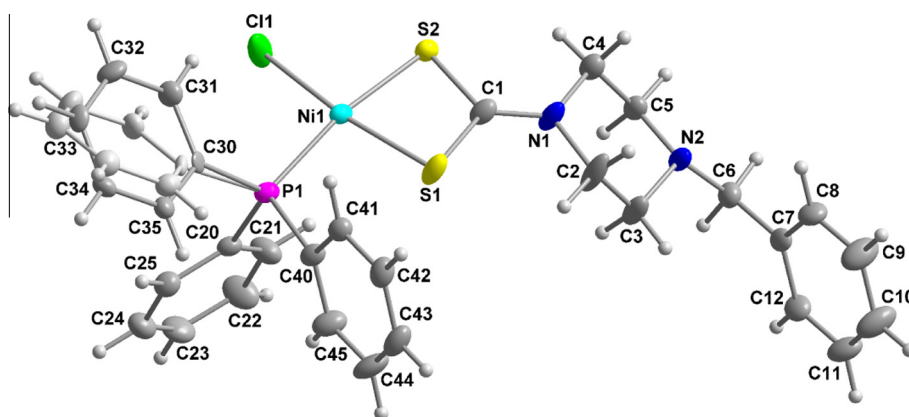


Fig. 1. The molecular structure of $[\text{NiCl}(\text{bpdtc})(\text{PPh}_3)]$ (**1**) with non-hydrogen atoms drawn as thermal ellipsoids at the 50% probability level. One phenyl ring of the PPh_3 molecule, involving C30–C35, is distorted over two positions with occupancy factors of 0.520(5) and 0.480(5).

those deposited in CSD for 86 nickel(II) bis(dithiocarbamate) complexes (2.147–2.227 Å range, average value of 2.200 Å). The crystal structures of the complexes are stabilized by C–H \cdots Ni, C–H \cdots S and C–H \cdots C (for $[\text{Ni}(\text{bpdtc})_2]$; see Fig. S2 in Appendix A, Supplementary data) and C–H \cdots S (for $[\text{Ni}(\text{tmdtc})_2]$; see Fig. S3 in Appendix A, Supplementary data) non-covalent contacts, whose parameters are listed in Tables S2 and S3 in Appendix A, Supplementary data.

3.3. UV-Vis spectroscopic study

The presence of bands at 18400–20900 cm^{-1} (543–478 nm) in the diffuse-reflectance spectra of **1–8**, assignable to the $^1\text{A}_{1g} \rightarrow ^1\text{B}_{1g}$ transition of the square-planar nickel(II) complexes [18,31,32], together with diamagnetic properties, support the assumption of the square-planar arrangement in the vicinity of the metal centre. The maxima, which exceeded 28,000 cm^{-1} , may be connected with intraligand charge-transfer (CT) transitions within the S_2CN moiety [18,33]. Regarding the above mentioned maxima at 18400–20900 cm^{-1} , their positions are in good agreement with those detected in Me_2CO , MeCN and CHCl_3 spectra of **1–8**, but they differ from those detected in DMF and DMSO solutions of the studied nickel(II) complexes (Table 2, Figs. 3 and S4).

To better understand the different behaviour of the studied complexes in DMF and DMSO, a comparison of the solution spectra of complexes **1–8** in DMF and DMSO with the diffuse-reflectance and MeNO₂ and DMF solution spectra of the starting compounds $[\text{Ni}(\text{bpdtc})_2]$ (precursor of **1–4**) and $[\text{Ni}(\text{tmdtc})_2]$ (precursor of **5–8**) was performed. The obtained results showed the same maxima positions in the DMF and DMSO solution spectra of **1–8** as

compared with the mentioned starting compounds (Fig. 4). Similar electronic spectra to those of diffuse-reflectance and MeNO₂ and DMF solution spectra of $[\text{Ni}(\text{bpdtc})_2]$ and $[\text{Ni}(\text{tmdtc})_2]$ and DMF (or DMSO) solutions of **1** and **5**, which involved two maxima at 15000–16100 and 22100–24400 cm^{-1} , corresponding to the $^1\text{A}_{1g} \rightarrow ^1\text{A}_{2g}$ and $^1\text{A}_{1g} \rightarrow ^1\text{B}_{1g}$ transitions, were recently reported for the nickel(II) bis(alkyldithiocarbamate) complex $[\text{Ni}(\text{ndtc})_2]$ [34]. As for the second type of used starting compounds, i.e. $[\text{NiX}_2(\text{PPh}_3)_2]$, two maxima can be found both in the solid state and 10^{-2} M DMF solution spectra, however, the spectra differ mutually in the curve shapes and maxima positions (Fig. 4). This difference is most probably connected with the change in composition and/or stereochemistry due to the formation of differently solvated $[\text{NiX}_A(\text{solV})_B]$ species ($X = \text{Cl}^-$ or NCS^- ; $\text{solV} = \text{DMF}$, DMSO; with varying ratios of A/B). For example, $[\text{NiCl}(\text{DMF})_x]^+$ ($x = 1–3$) species were detected in the mass spectra of **1** and **5** (see below).

3.4. ESI mass spectrometry

ESI⁺ mass spectra of **1**, **4**, **5** and **8** in Me_2CO , MeCN, MeOH, DMF, CHCl_3 , MeNO₂ and a MeOH/ H_2O mixture were recorded. All spectra (except for the MeOH/ H_2O mixture) contained peaks corresponding to $[\text{Ni}(\text{ndtc})(\text{PPh}_3)]^+$ (m/z 571.2 for **1** and **4**; m/z 498.2 for **5** and **8**) and $[\text{Ni}(\text{ndtc})(\text{PPh}_3)_2]^+$ (m/z 832.9 for **1** and **4**; m/z 760.1 for **5** and **8**) species. The Me_2CO , MeCN and DMF spectra involved peaks assignable to $[\text{Ni}(\text{solV})(\text{ndtc})(\text{PPh}_3)]^+$, where solV stands for the molecule of the mentioned solvent [35]. The species $[\text{Ni}(\text{solV})(\text{ndtc})(\text{PPh}_3)_2]^+$ were detected only in MeCN solutions, while the $[\text{Ni}(\text{ndtc})(\text{PPh}_3)_3]^+$ species (m/z 1170.0 for **1** and **4**; m/z

Table 3

Selected bond lengths (Å) and angles (°) of two crystallographically independent halves of $[\text{Ni}(\text{bpdtc})_2]$ (symmetry code: i - x , - y , - z), $[\text{Ni}(\text{tmdtc})_2]$ (symmetry code: i - x , - y , - z) and $[\text{NiCl}(\text{bpdtc})(\text{PPh}_3)]$ (**1**) determined by a single-crystal X-ray analysis.

Parameter	X-ray analysis		
	$[\text{NiCl}(\text{bpdtc})(\text{PPh}_3)]$ (1)	$[\text{Ni}(\text{bpdtc})_2]^a$	$[\text{Ni}(\text{tmdtc})_2]$
Ni1–S1	2.1724(7)	2.2007(13)/ 2.2013(13)	2.1996(5)
Ni1–S2	2.2181(6)	2.1967(13)/ 2.1983(13)	2.2074(5)
Ni1–S1 ⁱ	–	2.2007(13)/ 2.2012(13)	2.1997(5)
Ni1–S2 ⁱ	–	2.1968(13)/ 2.1982(13)	2.2075(5)
Ni1–P1	2.2029(6)	–	–
Ni1–Cl1	2.1627(7)	–	–
S1–C1	1.729(2)	1.699(5)/1.740(5)	1.723(2)
S2–C1	1.706(2)	1.717(5)/1.731(5)	1.717(2)
C1–N1	1.309(3)	1.309(6)/1.309(6)	1.318(2)
S1–Ni1–S2	78.60(2)	79.70(5)/79.78(5)	79.08(2)
S1–Ni1–S1 ⁱ	–	180.0/180.0	180.0
S1–Ni1–S2 ⁱ	–	100.30(5)/100.22(5)	100.92(2)
S2–Ni1–S1 ⁱ	–	100.30(5)/100.22(5)	100.92(2)
S2–Ni1–S2 ⁱ	–	180.0/180.0	180.0
S1 ⁱ –Ni1–S2 ⁱ	–	79.70(5)/79.78(5)	79.08(2)
S1–Ni1–P1	93.94(2)	–	–
S1–Ni1–Cl1	170.27(3)	–	–
S2–Ni1–P1	170.37(2)	–	–
S2–Ni1–Cl1	91.97(2)	–	–
P1–Ni1–Cl1	95.15(2)	–	–
Ni1–S1–C1	86.90(8)	84.7(2)/85.5(2)	85.83(7)
Ni1–S2–C1	86.00(8)	84.4(2)/85.8(2)	85.72(6)
S1–C1–N1	124.5(2)	125.2(4)/125.0(4)	124.89(14)
S2–C1–N1	127.4(2)	123.7(4)/126.2(4)	125.82(14)

^a Values of two crystallographically independent halves of molecules within the unit cell.

1022.0 for **5** and **8**) were identified in MeNO_2 (**1** and **4**) or MeCN (**5** and **8**) solutions (Fig. 5, S5–7). However, the situation was different in the DMF solution because the intensities of the $[\text{Ni}(\text{ndtc})(\text{PPh}_3)]^+$,

$[\text{Ni}(\text{solv})(\text{ndtc})(\text{PPh}_3)]^+$ and $[\text{Ni}(\text{ndtc})(\text{PPh}_3)_2]^+$ peaks significantly decreased as compared with the mass spectra in other solvents, and the strong peaks corresponding to $[\text{NiCl}(\text{DMF})_x]^+$ ($x = 1–3$, m/z 165.9, 238.9 and 311.7) and the low-intense peaks assignable to $[\text{Ni}(\text{bpdtc})(\text{DMF})_2]^+$ (m/z 454.8), $[\text{Ni}(\text{bpdtc})_2]^+$ (m/z 560.1; which may result from the in-source oxidation during the electrospray ionization) and $[(\text{Ni}(\text{bpdtc})_2)_2\text{Ni}(\text{bpdtc})]^+$ (m/z 868.9) species appeared in the DMF solution mass spectra (Figs. 5, S5 and S8). The mass spectra obtained in the $\text{MeOH}/\text{H}_2\text{O}$ mixture contained

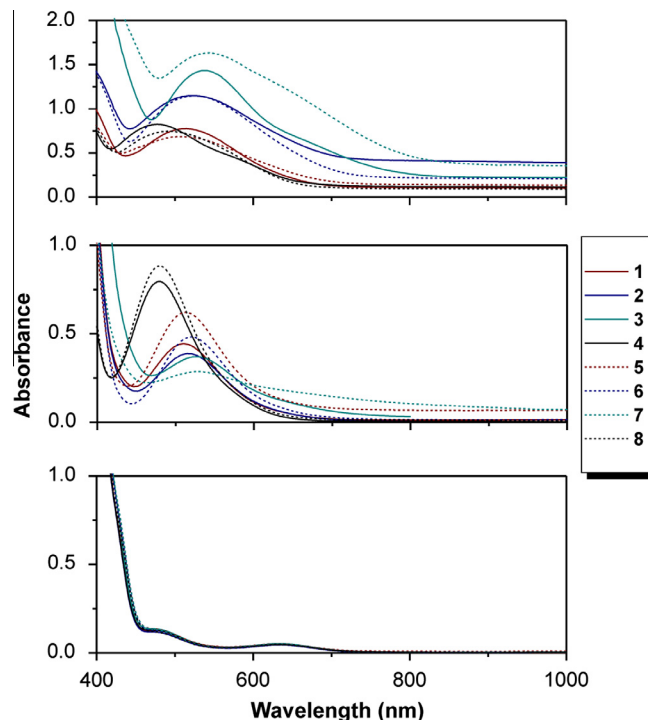


Fig. 3. The diffuse-reflectance (up) and electronic absorption spectra of 10^{-3} M MeNO_2 solutions (middle) and 10^{-3} M DMF solutions (down) of complexes **1–8**.

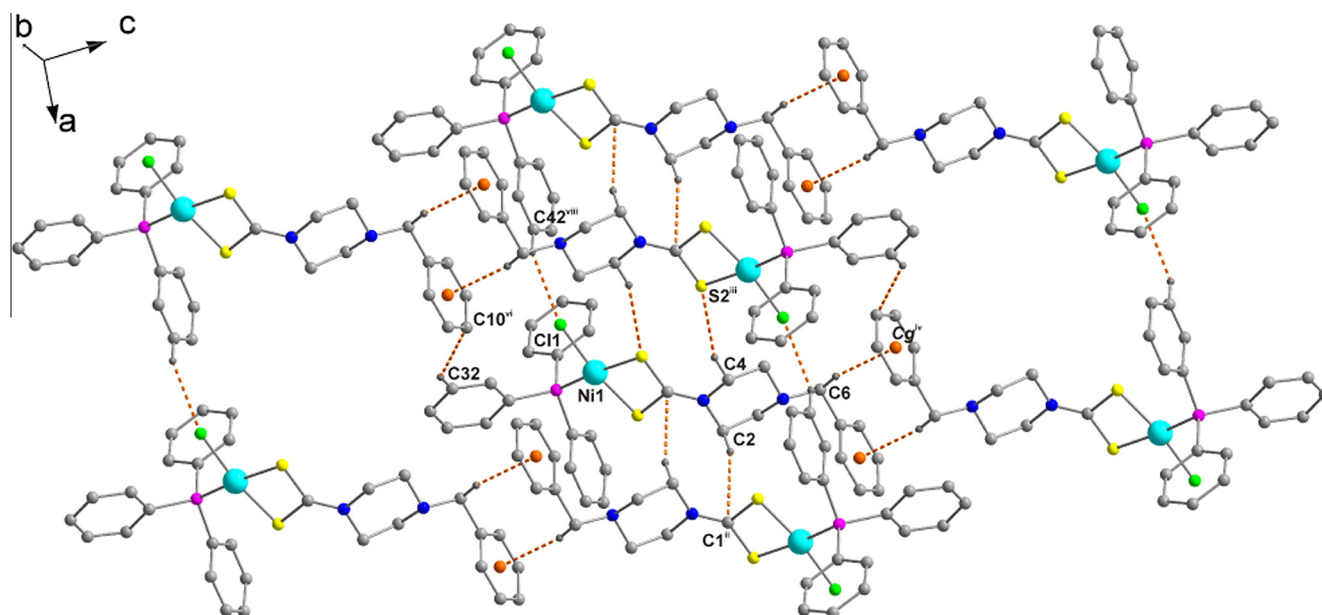


Fig. 2. Part of the crystal structure of $[\text{NiCl}(\text{bpdtc})(\text{PPh}_3)]$ (**1**) with the C2–H2B...C1, C4–H4B...S2, C6–H6A...Cg, C32–H32A...C10 and C42–H42A...C11 non-covalent contacts; the hydrogen atoms not involved in the depicted non-covalent contacts are omitted for clarity. Symmetry codes: (ii) $-x + 1$, $-y$, $-z + 1$; (iii) $-x$, $-y$, $-z + 1$; (iv) $-x + 1$, $-y$, $-z + 2$; (vi) $x - 1$, y , $z - 1$ and (viii) $x - 1$, y , z .

only the peaks corresponding to the $[\text{NiCl}(\text{H}_2\text{O})_x]^+$ species ($x = 2-5$) and PPh_3 (Figs. 5 and S5).

3.5. ^{31}P NMR spectroscopy

The signals of the coordinated PPh_3 molecules of complexes **1-8** were detected at 20.7–44.3 ppm (Table 2) in the ^{31}P NMR spectra measured in CDCl_3 solution. The differences in chemical shifts between the $[\text{NiX}(\text{bpdtc})(\text{PPh}_3)]$ (**1-4**; 20.7–29.4 ppm) and $[\text{NiX}(\text{tmdtc})(\text{PPh}_3)]$ (**5-8**; 34.0–44.3 ppm) complexes may be caused by a different value of the back bonding interaction of both

the respective *ndtc* anions. As for the *X* ligands within the structures of $[\text{NiX}(\text{ndtc})(\text{PPh}_3)]$, where $X = \text{Cl}^-$ (**1, 5**), Br^- (**2, 6**), I^- (**3, 7**) or NCS^- (**4, 8**), they deshield the phosphorus atom as well. As a consequence of these facts, the chemical shifts differ not only between the groups of complexes **1-4** and **5-8** (due to the *ndtc* anion), but also within each of the discussed groups (due to the *X* anion). A similar phenomenon was described in the literature for the $[\text{NiX}(\text{ndtc})(\text{PPh}_3)]$ type of compounds, where the mentioned ligands showed a deshielding ability as follows: $\text{NCS}^- > \text{Cl}^-$ [25] and $\text{Cl}^- > \text{NCS}^- > \text{Br}^- > \text{I}^-$ [23,36].

In the case of the spectra measured in $\text{DMSO}-d_6$ solutions of **1** and **5**, the chemical shift of PPh_3 in the ^{31}P NMR spectra corresponded to free non-coordinated PPh_3 molecules (−6.8 ppm for free PPh_3 ; −6.7 ppm for complex **1** and −6.3 ppm for complex **5**), while no signal in the above-mentioned region typical for a coordinated PPh_3 molecule was detected.

4. Conclusion

This work reports the preparation and thorough characterization of nickel(II) dithiocarbamates of the composition $[\text{NiX}(\text{ndtc})(\text{PPh}_3)]$ (*ndtc* stands for benzylpiperazine-dithiocarbamate (*bpdtc*; **1-4**) and thiomorpholine-dithiocarbamate (*tmdtc*; **5-8**); $X = \text{Cl}^-$, Br^- , I^- , NCS^-). The X-ray structure of complex **1** proved the distorted square-planar geometry of the complex. In an effort to elucidate the solution properties of the complexes, the representatives **1, 4, 5** and **8** were studied to determine their behaviour in different solvents in more detail. The complexes were found to be stable in Me_2CO , MeCN , MeOH , CHCl_3 and MeNO_2 . However, their stability was considerably lowered in DMF and DMSO, since the studied complexes decomposed to $[\text{Ni}(\text{ndtc})_2]$ and other undefined solvated Ni(II) species during their dissolution in these solvents. This work provides important evidence that the species in solution can significantly differ from those in solid state

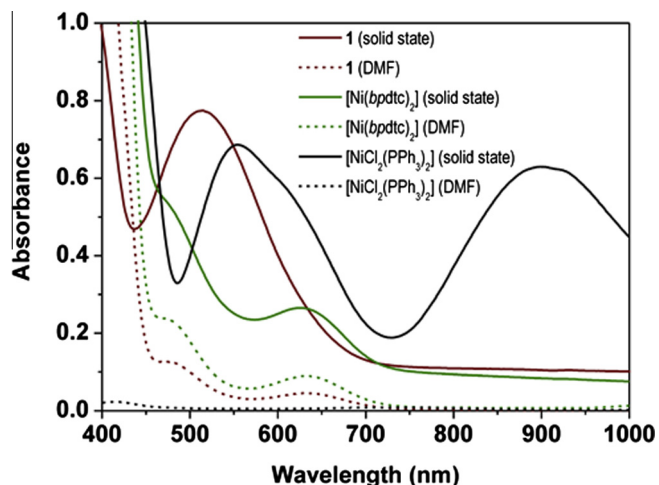


Fig. 4. Comparison of the electronic spectra of $[\text{NiCl}(\text{bpdtc})(\text{PPh}_3)]$ (**1**; red lines), $[\text{Ni}(\text{bpdtc})_2]$ (green lines) and $[\text{NiCl}_2(\text{PPh}_3)_2]$ (black lines) as recorded in the solid state (solid lines) and as DMF solutions (dashed lines), showing the similarity or differences in the stereochemistry of the studied complexes. (Color online.)

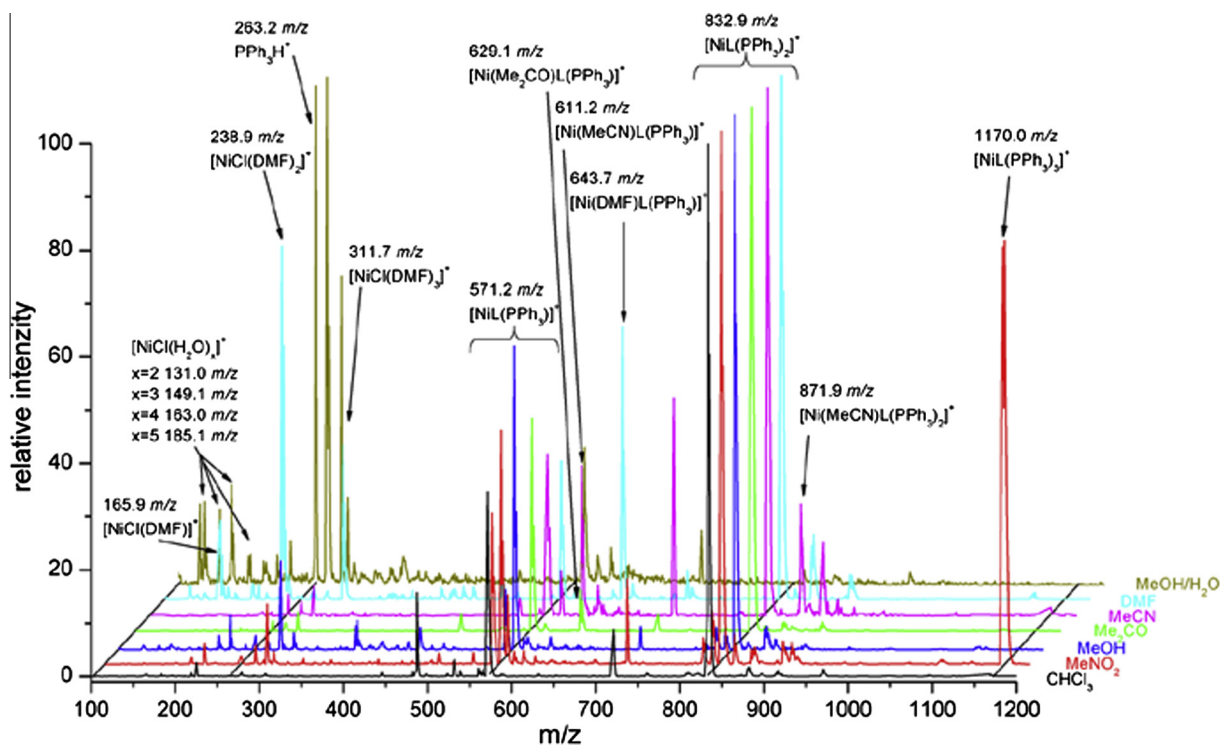


Fig. 5. ESI+ mass spectra of chloroform (CHCl_3 , black line), nitromethane (MeNO_2 , red line), methanol (MeOH , blue line), acetone (Me_2CO , green line), acetonitrile (MeCN , magenta line), *N,N'*-dimethylformamide (DMF, light blue line) and methanol/water (1:1 v/v, $\text{MeOH}/\text{H}_2\text{O}$, dark yellow line) solutions of **1** together with a description of the species corresponding to the most important peaks ($L = \text{bpdtc}$). (Color online.)

and thus, the solution behaviour of nickel dithiocarbamate complexes of the type $[\text{NiX}(\text{ndtc})(\text{PPh}_3)]$ has to be taken into account in connection with any possible practical application, e.g. a study of biological activity (usually done in DMSO, DMF and/or H_2O).

Acknowledgements

This research was supported by the Operational Program Research and Development for Innovations – European Regional Development Fund (CZ.1.05/2.1.00/03.0058), the Operational Program Education for Competitiveness – European Social Fund (CZ.1.07/2.3.00/20.0017) and by Palacký University (PrF_2013_015 and PrF_2012_009). The authors wish to thank Dr. Igor Popa for carrying out NMR measurements and Mr. Tomáš Šilha for performing CHN elemental analyses.

Appendix A. Supplementary data

The tables of the parameters of non-covalent contacts of $[\text{NiCl}(\text{bpdtc})(\text{PPh}_3)]$ (**1**; Table S1), $[\text{Ni}(\text{bpdtc})_2]$ (Table S2) and $[\text{Ni}(\text{tmdtc})_2]$ (Table S3), molecular structures of $[\text{Ni}(\text{bpdtc})_2]$ and $[\text{Ni}(\text{tmdtc})_2]$ (Fig. S1), part of the crystal structure of $[\text{Ni}(\text{bpdtc})_2]$ (Fig. S2) and $[\text{Ni}(\text{tmdtc})_2]$ (Fig. S3), UV–Vis spectra of **1–8** in different solvents and in the solid state (Fig. S4), ESI+ mass spectra **5** as observed in different solvents (Fig. S5), ESI+ mass spectra of the acetonitrile solutions of **1** and **4** (Fig. S6) and **5** and **8** (Fig. S7) and comparison of ESI+ mass spectra of DMF solutions of $[\text{Ni}(\text{bpdtc})_2]$, $[\text{NiCl}_2(\text{PPh}_3)_2]$ and complex **1** (Fig. S8) are given in Appendix A. CCDC 958805–958807 contain the supplementary crystallographic data for $[\text{NiCl}(\text{bpdtc})(\text{PPh}_3)]$ (**1**), $[\text{Ni}(\text{bpdtc})_2]$ and $[\text{Ni}(\text{tmdtc})_2]$, respectively. These data can be obtained free of charge via <http://www.ccdc.cam.ac.uk/conts/retrieving.html>, or from the Cambridge Crystallographic Data Centre, 12 Union Road, Cambridge CB2 1EZ, UK; fax: +44 1223 336 033; or e-mail: deposit@ccdc.cam.ac.uk. Supplementary data associated with this article can be found, in the online version, at <http://dx.doi.org/10.1016/j.poly.2013.11.041>.

References

- [1] D.J. Harding, P. Harding, S. Dokmairisrijan, H. Adams, Dalton Trans. 40 (2011) 1313.
- [2] A. Husain, S.A.A. Nami, S.P. Singh, M. Oves, K.S. Siddiqi, Polyhedron 30 (2011) 33.
- [3] C. Marzano, L. Ronconi, F. Chiara, M.C. Giron, I. Faustinelli, P. Cristofori, A. Trevisan, D. Fregona, Int. J. Cancer 129 (2011) 487.
- [4] S. Saeed, N. Rashid, R. Hussain, J.P. Jasinski, A.C. Keeley, S. Khan, J. Coord. Chem. 66 (2013) 126.
- [5] H. Cesur, T.K. Yazicilar, B. Bati, V.T. Yilmaz, Synt. React. Inorg. Met.-Org. Chem. 31 (2001) 1271.
- [6] Z. Trávníček, R. Pastorek, V. Slovák, Polyhedron 27 (2008) 411.
- [7] G. Marcotrigiano, G.C. Pellacani, C. Preti, J. Inorg. Nucl. Chem. 36 (1974) 3709.
- [8] C. Preti, G. Tosi, P. Zannini, Trans. Met. Chem. 4 (1979) 360.
- [9] K. Unoura, A. Yamazaki, A. Nagasawa, Y. Kato, H. Itoh, H. Kudo, Y. Fukuda, Inorg. Chim. Acta 269 (1998) 260.
- [10] Z. Trávníček, P. Štarha, R. Pastorek, J. Mol. Struct. 1049 (2013) 22.
- [11] F.A. Allen, Acta Crystallogr., Sect. B 58 (2002) 380.
- [12] Gmelins Handbuch der Anorganischen Chemie, Nickel, Teil C, Lief. 2, Verlag Chemie, GmbH, Weinheim, 1969, p. 1043.
- [13] E. König, Landolt-Börnstein, Springer, Berlin, 1966.
- [14] CRYSA LIS CCD and CRYSA LIS RED, Version 1.171.33.52 Oxford Diffraction Ltd., England, 2009.
- [15] G.M. Sheldrick, Acta Crystallogr., Sect. A 64 (2008) 112.
- [16] K. Brandenburg, DIAMOND, Release 3.1f, Crystal Impact GbR, Bonn, Germany, 2006.
- [17] W.J. Geary, Coord. Chem. Rev. 7 (1971) 81.
- [18] C.A. Tsipis, D.P. Kessissoglou, G.A. Katsoulos, Chim. Chron. New Ser. 14 (1985) 195.
- [19] S.V. Larionov, L.A. Patrino, I.M. Oglezneva, E.M. Uskov, Koord. Khim. 10 (1984) 92.
- [20] I.E. Černikova, I.A. Charonik, D.S. Umrejko, A.B. Kavrikov, V.I. Afanov, Koord. Khim. 15 (1989) 1695.
- [21] R. Pastorek, J. Kameníček, Z. Trávníček, Z. Šindelář, F. Březina, S. Sobancová, Nat. Chem. 133 (1994) 11.
- [22] R. Baskaran, K. Ramalingam, R. Thirunelakandan, B.A. Prakasam, G. Bocelli, A. Cantoni, J. Coord. Chem. 62 (2009) 1076.
- [23] R. Pastorek, J. Kameníček, J. Husárek, V. Slovák, M. Pavlíček, J. Coord. Chem. 60 (2007) 485.
- [24] K. Ramalingam, G. Aravamudan, M. Seshasayee, C. Subramanyam, Acta Crystallogr., Sect. C 40 (1984) 965.
- [25] R. Pastorek, J. Kameníček, F. Březina, J. Lasovský, Z. Šindelář, J. Ondráček, Nat. Chem. 32 (1993) 7.
- [26] R. Pastorek, Z. Trávníček, E. Kvapilová, Z. Šindelář, F. Březina, J. Marek, Polyhedron 18 (1999) 151.
- [27] R. Pastorek, J. Kameníček, Z. Trávníček, J. Husárek, N. Duffy, Polyhedron 18 (1999) 2879.
- [28] M. Pavlíček, Z. Trávníček, R. Pastorek, J. Marek, Transition Met. Chem. 28 (2003) 260.
- [29] A. Kropidłowska, J. Janczak, J. Golaszewska, B. Becker, Acta Crystallogr., Sect. E 63 (2007). m1947-u1444.
- [30] A. Kropidłowska, J. Chojnacki, J. Golaszewska, B. Becker, Acta Crystallogr. E63 (2007). m1643-u640.
- [31] A.B.P. Lever, Inorganic Electronic Spectroscopy, second ed., Elsevier, Amsterdam, 1984.
- [32] C.A. Tsipis, D.P. Kessissoglou, G.E. Manoussakis, Inorg. Chim. Acta 65 (1982) L137.
- [33] C.A. Tsipis, I.E. Meleziadis, D.P. Kessissoglou, G.A. Katsoulos, Inorg. Chim. Acta 90 (1984) L19.
- [34] S. Bajja, A. Mishra, J. Coord. Chem. 64 (2011) 2727.
- [35] K. Jiang, G. Bian, Y. Chai, H. Yang, Q. Lai, Y. Pan, Int. J. Mass Spectrom. 321 (2012) 40.
- [36] Z. Trávníček, R. Pastorek, P. Štarha, I. Popa, V. Slovák, Z. Anorg. Allg. Chem. 636 (2010) 1557.